Journal of ELECTRONIC MATERIALS, Vol. 44, No. 10, 2015
DOI: 10.1007/s11664-015-3880-8


# High-Performance Simultaneous Two-Photon Absorption Upconverted Stimulated Single-Component $Sr_2V_2O_7$ Phosphor for White LEDs

HONG PAN,[1] LEI ZHANG,[1] LONG JIN,[1] BINBIN ZHANG,[1] and WEIQING YANG[1,2,3]

1.—Key Laboratory of Advanced Technologies of Materials (Ministry of Education), School of Materials Science and Engineering, Southwest Jiaotong University, Chengdu 610031, China. 2.—State Key Laboratory of Electronic Thin Films and Integrated Devices, University of Electronic Science and Technology of China, Chengdu 610054, China. 3.—e-mail: wqyang@swjtu.edu.cn

Notwithstanding the wide use of white light-emitting diodes (w-LEDs), conventionally consisting of multiple emitting components, some inevitable issues still exist nowadays, such as the intrinsic color balance, device complexity, and high cost associated with such multiple emitting components. We have synthesized simultaneous two-photon absorption upconverted stimulated single-component $Sr_2V_2O_7$ phosphor for use in w-LEDs. Due to the photon avalanche upconversion, the as-grown phosphor exhibits an enhanced photoluminescence spectrum in the range of 400 nm to 650 nm for white light when excited by red light at 693 nm. Moreover, when evenly dispersed in polyethylene glycol dispersant, the as-grown phosphor simultaneously produced strong visible white light when using an excitation wavelength $\lambda_{ex}$ of 693 nm, suggesting a possible route to produce w-LEDs by using red chips as an excellent substitute for traditional w-LEDs with multiple emitting components based on rare-earth metals. Finally, density functional calculations were performed using the generalized gradient approximation to study the electronic structure of $Sr_2V_2O_7$ crystal. A reasonable model is proposed to explain the two-photon absorption luminescence mechanism.

**Key words:** White light-emitting diodes, single-component phosphors, $Sr_2V_2O_7$, two-photon absorption

## INTRODUCTION

Recently, upconverted (UC) stimulated inorganic fluorides have attracted considerable attention due to their unique optical properties for potential applications in diverse fields such as biological labeling, solar spectral conversion, and imaging.[1–7] Meanwhile, single-component white-light phosphors for use in white light-emitting diodes (w-LEDs) have also become attractive as they avoid many issues associated with the use of multiple emitting phosphors, such as the intrinsic color balance, device complexity, and high cost.[8–12] To date, work on single-component white-light phosphors has mainly focused on downconverted (DC) inorganic fluorides stimulated by ultraviolet (UV) light,[8–16] in which the stronger UV light and the weaker or even no red light results in a lower color temperature and thus poorer color rendering index for w-LEDs. If the UC mode excited by red or near-infrared (NIR) LED chips could be applied with single-component phosphors to make up for the lack of red light from traditional w-LEDs,[8–12] their further development could be greatly promoted.

Herein, we present a simultaneous two-photon absorption (TPA) UC stimulated single-component

(Received November 22, 2014; accepted May 30, 2015; published online June 17, 2015)

$Sr_2V_2O_7$ (SVO) phosphor with an emission spectrum in the range of 400 nm to 650 nm that can be effectively excited by red light at 693 nm to produce white LEDs. Furthermore, the as-grown phosphor was dispersed in polyethylene glycol at low concentration of 1.0 mg/mL, and this kind of phosphor could simultaneously produce luminous white light when excited by red light at 693 nm, unambiguously demonstrating a promising method for commercial application of single-component phosphors for w-LEDs. Lastly, using density functional theory calculations based on the generalized gradient approximation (GGA),[17] the bandgap $E_g$ and pseudogap $E_{pg}$ were proved to be $3.453 \pm 0.003$ eV and $1.876 \pm 0.006$ eV, respectively, from the band structure and partial density of states (PDOS) results for SVO crystal. A TPA model is constructed to explain the luminescence mechanism of the upconverted stimulated SVO phosphor for use in white LEDs.

## METHODS

### Experimental Procedures

Single-component white-light SVO phosphor with dual-mode excitation was synthesized by the traditional solid-state reaction method with $SrCO_3$ (99.5%) and $NH_4VO_3$ (99.9%) (Changzheng Chemical Reagent Company, China) as source materials. Starting materials according to the stoichiometric phosphor composition were mixed homogeneously in an agate mortar, then annealed in the range of 1000°C for 3 h.

A DX 2700 x-ray diffractometer (XRD) with Cu $K_\alpha$ radiation ($\lambda$ = 0.15418 nm) was used to determine the crystal structures of the as-grown SVO phosphor. The corresponding data were collected over the $2\theta$ range from 15° to 60° in steps of 0.02° with counting time of 2 s per step. Moreover, the morphology and composition of the as-grown phosphor were examined by scanning electron microscopy (SEM, S4800) and energy-dispersive x-ray spectroscopy (EDS, S4800), respectively. Finally, the photoluminescence (PL) and Fourier-transform infrared (FTIR) spectra of the as-grown phosphor were investigated at room temperature using a Shimadzu RF-5301PC spectrofluorometer with a 150-W xenon lamp as excitation energy source and a Shimadzu RF-IRPrestige-21 spectrometer, respectively.

### Theoretical Methods

Density functional theory calculations were carried out using the generalized gradient approximation (GGA)–Perdew–Burke–Ernzerhof (PBE) method[17] to study the electronic structure of SVO crystal. The full-potential projector augmented wave (PAW)[18,19] method implemented in the Vienna *ab initio* Simulation Package (VASP)[20,21] was applied for the calculations. To ensure the accuracy of the electronic

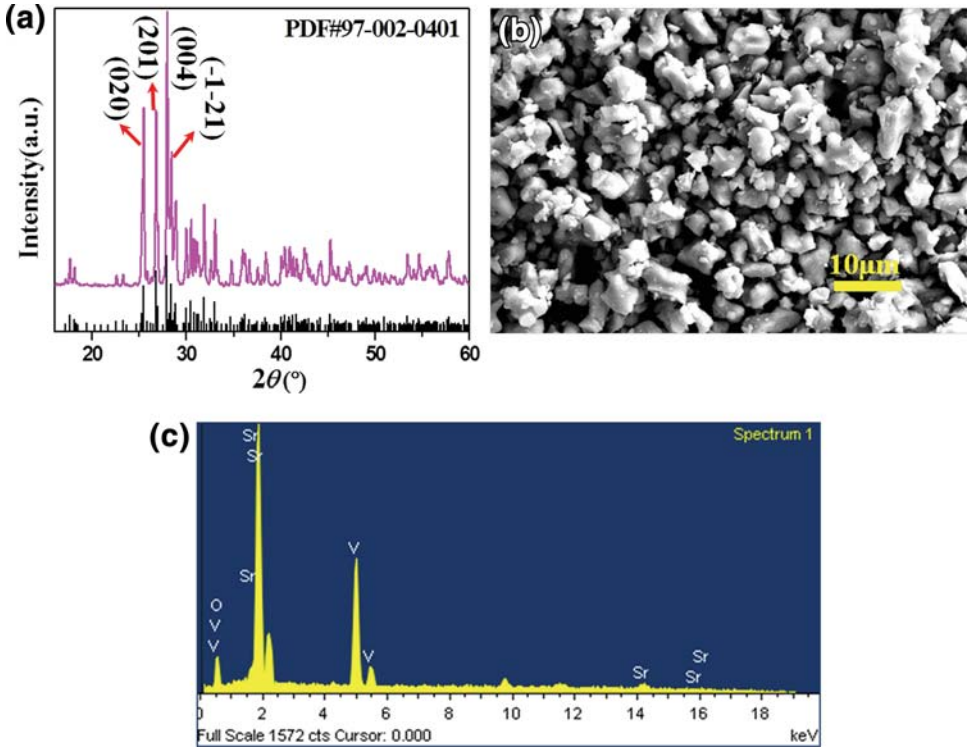


Fig. 1. Crystal structure and surface topography of as-grown $Sr_2V_2O_7$ phosphor: (a) XRD pattern, (b) SEM image, and (c) EDS of $Sr_2V_2O_7$ phosphor.

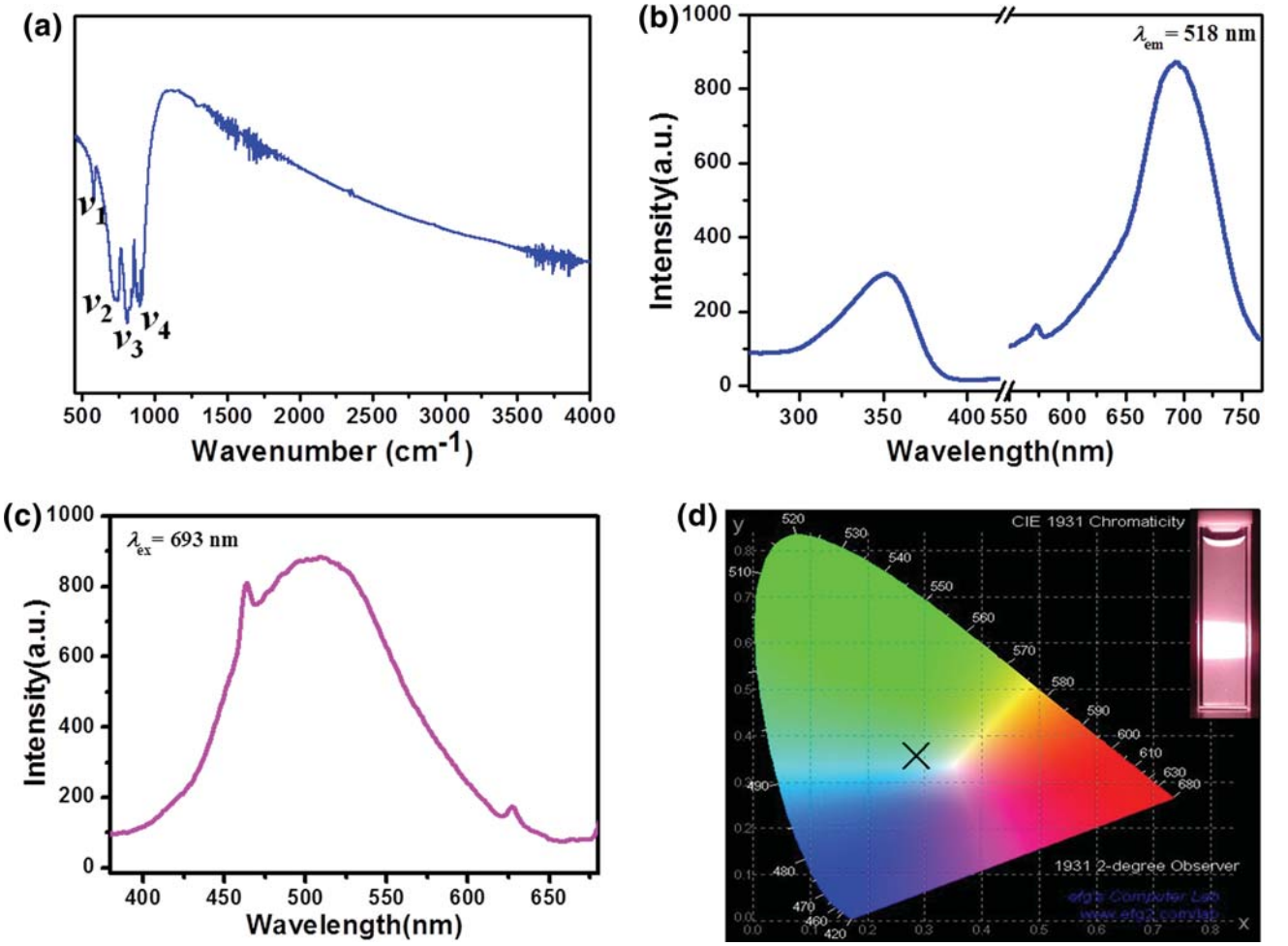


Fig. 2. Optical properties of as-grown $Sr_2V_2O_7$ phosphor: (a) FTIR spectra, (b) PLE spectra, (c) PL spectra, and (d) photograph and corresponding CIE chromaticity coordinates of $Sr_2V_2O_7$ phosphor dispersed in polyethylene glycol for $\lambda_{ex}$ = 693 nm.

calculations, the Brillouin zone samplings used $2 \times 2 \times 2$ $k$-point grids for the primitive cell, the self-consistent field (SCF) energy convergence threshold was set at $10^{-6}$ eV/atom, and the cutoff energy for the plane-wave basis was selected as 500 eV.

## RESULTS AND DISCUSSION

### Crystal Structure and Morphology

The crystal structure of the as-grown phosphor is described in detail in Fig. 1, in which the XRD pattern (Fig. 1a) of the SVO phosphor agrees well with literature data (PDF#97-002-0401).[22] Additionally, the SEM image of the SVO phosphor in Fig. 1b shows that the SVO crystalline grains are approximately spherical with average diameter of around 2 $\mu$m to 5 $\mu$m, matching well with the optimal size and shape required for encapsulation of white LEDs.[23,24] Furthermore, the $N_{Sr}$:$N_V$:$N_O$ atomic ratio as characterized by EDS was found to be 19.53:19.78:68.55 $\approx$ 2:2:7 (Fig. 1c), excellently matching the nominal stoichiometry of the SVO phosphor and indicating that our experimental results can be considered reasonable.

The FTIR spectrum of the as-grown phosphor is shown in Fig. 2a. There are four FTIR spectral peaks, located at $v_1$ = 581 cm$^{-1}$, $v_2$ = 748 cm$^{-1}$, $v_3$ = 813 cm$^{-1}$, and $v_4$ = 897 cm$^{-1}$, which can be assigned to stretch vibrations of $VO_4$ dimers.[25–29] As shown in Fig. 2a, the absorption peaks at $v_1$ = 581 cm$^{-1}$ and $v_2$ = 748 cm$^{-1}$ should originate from V–O–V bridge vibrations and asymmetric stretching of longer V–O bond,[27–29] respectively. The others can mainly be ascribed to symmetric stretching of the three other shorter V–O bonds.[27–29]

### Photoluminescence Properties

For further understanding of the photoluminescence properties, the photoluminescence excitation (PLE) spectrum of the as-grown phosphor was obtained using an emission wavelength $\lambda_{em}$ of 518 nm. As shown in Fig. 2b, the PLE spectrum of the SVO phosphor consisted of two broad band peaks in the ranges of 300 nm (4.140 eV) to 380 nm (3.269 eV) and 600 nm (2.070 eV) to 760 nm

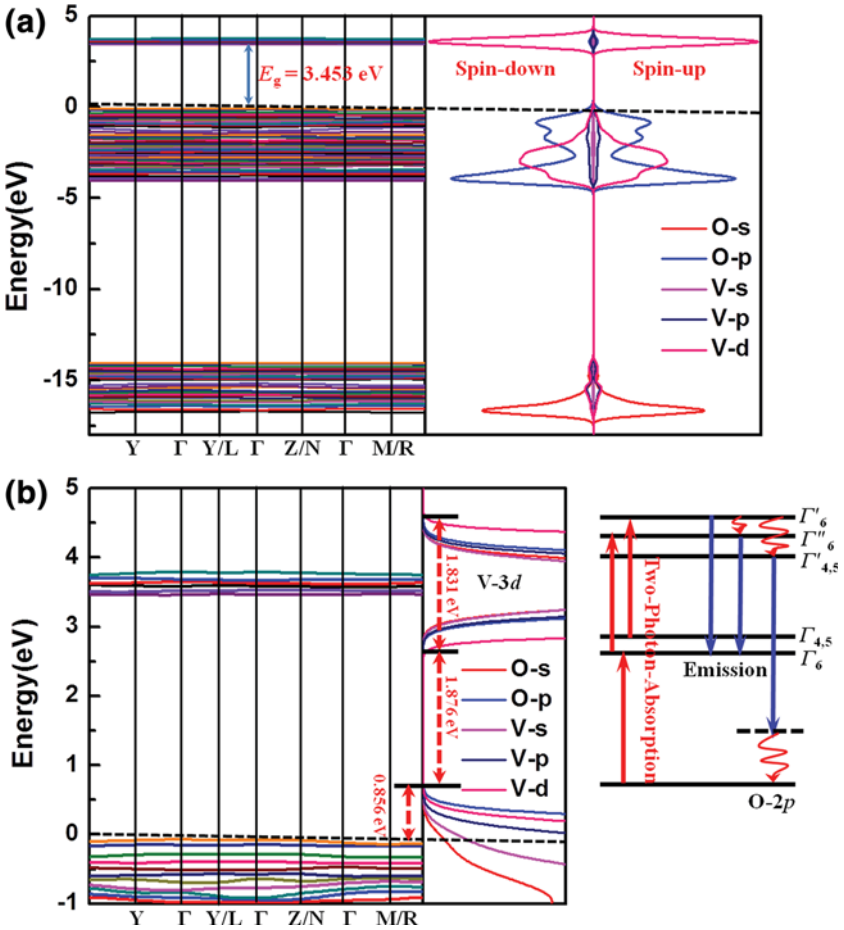


Fig. 3. Electronic structure and photoluminescence mechanism of $Sr_2V_2O_7$ phosphor: (a) band structure (left) and partial density of states (right) of as-grown $Sr_2V_2O_7$, (b) enlarged band structure (left), partial density of states (middle), and two-photon absorption mechanism (right) of upconverted stimulated $Sr_2V_2O_7$ phosphor for use in white LEDs.

(1.635 eV). The energy of the former is exactly two times that of the latter. The former broad band peak is mainly ascribed to $V^{5+}$–$O^{2-}$ charge transfer (CT).[13,14,23,30–36] The latter can only be effectively stimulated in the PL spectrum of the SVO phosphor by simultaneous absorption of two photons, i.e., two-photon absorption (TPA). Therefore, red light at 693 nm was used to excite the SVO phosphor, and the corresponding PL spectrum is shown in Fig. 2c, showing an obvious broadening of the white-light spectrum in the range of about 400 nm to 650 nm, evidently predicting that the SVO phosphor could effectively emit enhanced UC-mode white light when excited at 693 nm.

To intuitively reveal the fluorescence performance of the SVO phosphor, we evenly dispersed the as-grown phosphor in polyethylene glycol dispersant at low concentration of 0.1 mg/mL. From Fig. 2d, it is obvious that the photoluminescence of the mixture with the SVO phosphor showed bright visible white light for the excitation wavelength $\lambda_{ex}$ of 693 nm. Additionally, the corresponding Commission Internationale de l'Éclairage (CIE) chromaticity coordinates (0.281, 0.356) are very close to the correct values for white light, suggesting that SVO is a potential UC stimulated single-component phosphor for use in white LEDs.

## Electronic Structure and Photoluminescence Mechanism

In this section, we present the band structure, PDOS, and photoluminescence mechanism of the as-grown SVO phosphor. Figure 3a shows the band structure of SVO crystal and the PDOS of V and O elements. These results reveal that SVO crystal has a bandgap $E_g$ of approximately 3.453 ± 0.003 eV at the Γ point, in good agreement with the one-photon absorption excitation wavelength of 355 nm (3.499 eV) (Fig. 2b). According to the PDOS spectra in Fig. 3a (right) and the locally enlarged PDOS spectra in Fig. 3b (middle), the top of the valence band (VB) close to 0 eV is dominated by O 2*p* orbitals while the conduction band (CB) is controlled by V 3*d* orbitals. Remarkably, the O 2*p* orbital band edge appears at about 0.856 ± 0.002 eV above the Fermi level whereas that of the V 3*d* orbital expands $\Delta E$ = 0.721 ± 0.004 eV toward the Fermi

level. These band edges reveal that the pseudogap $E_{pg}$ should be about 1.876 ± 0.006 eV, which is very close to the excitation energy of 1.793 eV (693 nm).

Based on this, one can deduce the luminescence mechanism shown in Fig. 3b (right) for the simultaneous TPA upconverted stimulated single-component phosphor for use in white LEDs. As we know, the origin of the PLE spectrum would be the CT transition from the full 2*p* orbital of oxygen ligands to the vacant 3*d* orbital of $V^{5+}$ in approximately trigonal $VO_4$ with $C_{3v}$ symmetry.[13,14,23,30–36] The $d^0$ electronic configuration becomes the $d^1$ electronic configuration, then $V^{5+}O_4^{2-}$ changes to $V^{4+}O_4^{-}$.[35,36] More precisely, the spectral term $^2D$ of the $d^1$ electron configuration would split into the energy level irreducible expression $\Gamma_6$, $\Gamma_{4,5}$, $\Gamma'_{4,5}$, $\Gamma''_6$, and $\Gamma'_6$ due to the approximately trigonal $C_{3v}$ crystal field interaction plus the spin–orbit interaction.[33,34] The broad PLE peaks at 300 nm to 380 nm and 600 nm to 760 nm can be ascribed to $V^{5+}$–$O^{2-}$ CT after one-photon absorption (OPA) and TPA,[13,14,30–39] respectively. Meanwhile, the broad PL spectrum of the SVO phosphor mainly originates from both in-band transitions of $\Gamma'_6 \rightarrow \Gamma_6$ and $\Gamma''_6 \rightarrow \Gamma_6$ of $V^{4+}$ ions in $VO_4$ groups with approximately $C_{3v}$ symmetry and interband transitions of $3d \rightarrow 2p$ with participation of nonradiative relaxation. The reasoning above evidently implies that the broad emission of the SVO phosphor should result from both in-band and interband transitions of four different $VO_4$ groups with $C_{3v}$ symmetry. Interestingly, in Fig. S1, the UC luminescence intensities of the as-grown SVO phosphor are much higher than the DC luminescence intensities, mainly due to photon avalanche and TPA according to the transition probability.[40–42]

In summary, we successfully synthesized a kind of simultaneous TPA upconverted stimulated single-component $Sr_2V_2O_7$ phosphor for use in white LEDs. The UC luminescence intensities when excited by red light at 693 nm are much higher than the traditional DC luminescence intensities from samples excited by ultraviolet light at 355 nm, which is mainly attributed to photon avalanche and TPA effects. This kind of phosphor offers a promising approach for commercial applications of single-component phosphors in w-LEDs and represents a potential substitute material for the increasingly scarce rare-earth materials currently used in LED phosphors. We successfully constructed a TPA model to investigate the luminescence mechanism of the upconverted stimulated SVO phosphor for white LEDs, providing a potential method offering insight into the luminescence problems of similar phosphors.

## ACKNOWLEDGEMENTS

This work is supported by the National Natural Science Foundation of China (No. 51202023), Sichuan Province Science and Technology Plan Project (No. 2015JQ0013), and the Fundamental Research Funds for the Central Universities (A0920502051408-10).

## ELECTRONIC SUPPLEMENTARY MATERIAL

The online version of this article (doi: 10.1007/s11664-015-3880-8) contains supplementary material, which is available to authorized users.

## REFERENCES

1. Y.S. Liu, D.T. Tu, H.M. Zhu, R.F. Li, W.Q. Luo, and X.Y. Chen, *Adv. Mater.* 22, 3266 (2010).
2. F. Wang, Y. Han, C.S. Lim, Y. Lu, J. Wang, J. Xu, H. Chen, C. Zhang, M. Hong, and X.G. Liu, *Nature* 463, 1061 (2010).
3. G.G. Zhang, C.M. Liu, J. Wang, X.J. Kuang, and Q.J. Su, *Mater. Chem.* 22, 2226 (2012).
4. D.Q. Chen, Y.L. Yu, H. Lin, P. Huang, Z.F. Shan, and Y.S. Wang, *Opt. Lett.* 35, 220 (2010).
5. P. Li, Q. Peng, and Y.D. Li, *Adv. Mater.* 21, 1945 (2009).
6. D.Q. Chen, Y.L. Yu, F. Huang, H. Lin, P. Huang, A.P. Yang, Z.X. Wang, and Y.S. Wang, *J. Mater. Chem.* 22, 2632 (2012).
7. D.T. Tu, L.Q. Liu, Q. Ju, Y.S. Liu, H.M. Zhu, R.F. Li, and X.Y. Chen, *Angew. Chem. Int. Ed.* 50, 6306 (2011).
8. N. Guo, Y.J. Huang, M. Yang, Y.H. Song, Y.H. Zheng, and H.P. You, *Phys. Chem. Chem. Phys.* 13, 15077 (2011).
9. W. Ki and J. Li, *J. Am. Chem. Soc.* 130, 8114 (2008).
10. H.A. Höppe, M. Daub, and M.C. Bröhmer, *Chem. Mater.* 19, 6358 (2007).
11. M.S. Wang, S.P. Guo, Y. Li, J.P. Cai, G. Xu, W.W. Zhou, F.K. Zheng, and G.C. Guo, *J. Am. Chem. Soc.* 131, 13572 (2009).
12. S. Sapra, S. Mayilo, T.A. Klar, A.L. Rogach, and J.A. Sammons, *Adv. Mater.* 19, 569 (2007).
13. T. Nakajima, M. Isobe, T. Tsuchiya, Y. Ueda, and T. Kumagai, *Nat. Mater.* 7, 735 (2008).
14. T. Nakajima, M. Isobe, T. Tsuchiya, Y. Ueda, and T. Manabe, *J. Phys. Chem. C* 114, 5160 (2010).
15. R. Singh and S.J. Dhoble, *Bull. Mater. Sci.* 34, 557 (2011).
16. W.Q. Yang, Z.L. Liu, J. Chen, H. Li, L. Zhang, H. Pan, B. Wu, and Y. Lin, *Sci. Rep.* 5, 10460 (2015).
17. J.P. Perdew, K. Burke, and M. Ernzerhof, *Phys. Rev. Lett.* 77, 3865 (1996).
18. P.E. Blöchl, *Phys. Rev. B* 50, 17953 (1994).
19. G. Kresse and D. Joubert, *Phys. Rev. B* 59, 1758 (1999).
20. G. Kresse and J. Hafner, *Phys. Rev. B* 49, 14251 (1994).
21. G. Kresse and J. Furthmüller, *Comput. Mater. Sci.* 6, 15 (1996).
22. A.A. Vedernikov, YuA Velikodnyi, V.V. Ilyukhin, and V.K. Trunov, *Dok. Akad. Nauk SSSR* 263, 101 (1982).
23. W.Q. Yang, H.G. Liu, M. Gao, Y. Bai, J.T. Zhao, X.D. Xu, B. Wu, W.C. Zheng, G.K. Liu, and Y. Lin, *Acta Mater.* 61, 5096 (2013).
24. W.Q. Yang, H.G. Liu, G.K. Liu, Y. Lin, M. Gao, X.Y. Zhao, W.C. Zheng, Y. Chen, J. Xu, and L.Z. Li, *Acta Mater.* 60, 5399 (2012).
25. F.C. Hawthorne and C. Calvo, *J. Solid State Chem.* 22, 157 (1977).
26. S. Benmokhtar, A.E. Jazouli, J.P. Chaminade, P. Gravereau, F. Guillen, and D.D. Waal, *J. Solid State Chem.* 177, 4175 (2004).
27. B.V. Rao and S. Buddhudu, *Mater. Chem. Phys.* 111, 65 (2008).
28. A. Mer, S. Obbade, M. Rivenet, C. Renard, and F. Abraham, *J. Solid State Chem.* 185, 180 (2012).
29. V.R. Bandi, B.K. Grandhe, M. Jayasimhadri, K. Jang, H.S. Lee, S.S. Yi, and J.H. Jeong, *J. Cryst. Growth* 326, 120 (2011).
30. Y.L. Huang, Y.M. Yu, T.J. Tsuboi, and H.J. Seo, *Opt. Exp.* 20, 4360 (2012).

31. Y.S. Hu, W.D. Zhuang, H.Q. Ye, D.H. Wang, S.S. Zhang, and X.W. Huang, *J. Alloys Compd.* 390, 226 (2005).
32. Z. Ci, Y. Wang, J. Zhang, and Y. Sun, *Phys. B* 403, 670 (2008).
33. Z.L. Wang, H.B. Liang, and M.L. Gong, *J. Alloys Compd.* 432, 308 (2007).
34. C.J. Ballhausen, *Introduction to Ligand Field Theory* (New York: McGraw-Hill, 1962).
35. Q.L. Zhang, C.X. Guo, and C.S. Shi, *J. Lumin.* 21, 353 (2000).
36. Q.L. Zhang, C.X. Guo, C.S. Shi, Y.G. Wei, Z.M. Qi, and Y.J. Tao, *Chin. Rare Earth Soc.* 19, 1 (2001).
37. I.I. Karpov, B.N. Grechushnikov, and V.F. Koryagin, *Sov. Phys. Dokl.* 23, 492 (1978).
38. O.P. Agarwal and P. Chand, *Solid State Commun.* 52, 417 (1984).
39. W.Q. Yang and W.C. Zheng, *Spectrosc. Lett.* 44, 354 (2011).
40. M.K. Wermuth and H.U. Güdel, *J. Am. Chem. Soc.* 121, 10102 (1999).
41. S. Sivakumar, F.C.J. Veggel, and P.S. May, *J. Am. Chem. Soc.* 129, 620 (2007).
42. D.A. Fishman, C.M. Cirloganu, S. Webster, L.A. Padilha, M. Monroe, D.J. Hagan, and E.W. Stryland, *Nat. Photon.* 5, 561 (2011).